Structure of electromagnetic field excited by an electron bunch in a semi-infinite dielectric-filled waveguide

I. N. Onishchenko, D. Yu. Sidorenko, and G. V. Sotnikov
Institute of Plasma Electronics and New Methods of Acceleration, National Scientific Center "Kharkov Institute of Physics and Technology," 1 Akademicheskaya Street, Kharkov 61108, Ukraine
(Received 3 December 2001; published 10 June 2002)

The exact solution of a problem on electromagnetic field excitation by a thin annular charged bunch in a semi-infinite round cylindrical waveguide with metal sidewalls and solid homogeneous dielectric filling is obtained. Expressions for all components of electromagnetic field are derived. These formulas describe the excited field at any point and any moment of time. In contrast to previous works, where asymptotic methods (saddle-point technique) were used, we applied a number of successive conformal transformations of integration area in order to carry out the inverse Fourier transformation. Integration along the initial infinite straight-line contour was substituted by integration along the closed circular contour. This allowed us to separate out the integral presentation of the cylindrical Bessel function of first kind and obtain the final solution in the form of infinite converging series. The process of integration is presented in detail. Both cases, when the Cherenkov resonance condition is satisfied and when this condition is not satisfied, are considered. Spatial pictures of field excited by a finite-size electron bunch are calculated numerically and discussed. In the case of the Cherenkov resonance the drift of excited wake field after the bunch with group velocity is demonstrated, and in the nonresonance case the appearance of impulse of transition radiation and the presence of precursor of the signal are shown.

DOI: 10.1103/PhysRevE.65.066501 PACS number(s): 41.60.−m

I. INTRODUCTION

A round cylindrical waveguide with metal sidewalls and dielectric filling is often used in experiments on excitation of electromagnetic oscillations by electron bunches. The excited waves can be applied for wake-field acceleration of charged particles [1–5] or for radiation sources [6,7]. For a theoretical examination of field excited by moving charge in such waveguide it is usually supposed that a waveguide is infinite along the z axis. Consequently, if the Cherenkov resonance condition is satisfied, the excited field will be obtained in the form of the Cherenkov wave, which occupies the whole region behind the charge [8]. If there is no resonance, then only the exponentially decaying quasistatic field of moving charge can be obtained.

The semi-infinite waveguide, which is shorted with metal wall at the input end, can be considered as a first approximation for theoretical description of finite-length system without reflections. For the first time the field of uniformly moving point charge in such a waveguide was considered by Burshtein and Voskresenskij [9]. They presented the excited field as a sum of three components. The first component is the Cherenkov wave, the same as in an infinite waveguide. The second one is the ''quenching wave,'' which compensates the Cherenkov wave in the region between the face wall $z=0$ and the ''group wave front'' $z=v_{gr}t$, where v_{gr} is the group velocity of synchronous electromagnetic wave in the round dielectric-filled waveguide. The third component ensures smooth passage across the group wave front region. It corresponds to the transition radiation, which arises due to presence of boundary $z=0$ irrespective of satisfaction of Cherenkov resonance condition. This additional field was determined with the help of the saddle-point technique. The obtained approximate solution contains Fresnel integrals and is valid for the moments of time, which are large in comparison with the wave period.

Propagation of transition radiation can be described with the help of formalism, applied for study of pulsed signal propagation in dispersive medium. The expansion of phase of incoming signal in series [10,11] or asymptotic methods [12,13] were usually applied for that. In a number of particular cases of dispersive media with dispersion equation of the form $k_z \propto \sqrt{\omega^2-\omega_p^2}$, where k_z is the longitudinal wave number, ω is the wave frequency, ω_p is some critical frequency, the exact solutions were obtained: for the ionosphere by Denisov [14] and for the flat waveguide by Wait and Spies [15].

As the dispersion equation of round cylindrical metal waveguide with solid dielectric filling has similar form, there is the possibility to obtain exact solution for the field of transition radiation in such waveguide. So, in the present paper for approximation of prescribed uniform motion of charged bunch, the expressions for the field, which are valid at any point and any moment of time, will be derived. Based on these expressions the structure of field excited by electron bunch in the semi-infinite waveguide will be described.

This paper is organized as follows. Section II gives a detailed description of calculation of field of elementary thin charged ring. We considered in parallel the case when the Cherenkov resonance condition is satisfied, and the case when this condition is not satisfied. All values, which relate to the nonresonance case, are marked with tilde. In Sec. III the computed pictures of spatial two-dimensional (2D) distribution of field of finite-size electron bunch are presented and discussed.

II. FIELD OF A THIN CHARGED RING

A. Integral expressions for the field components

Consider the cylindrical metal waveguide with radius b, filled with homogeneous dielectric with relative dielectric constant ε. Along the longitudinal direction the waveguide is semi-infinite ($0 \leqslant z < \infty$), at the end $z=0$ it is shorted with a metal wall that is transparent for electrons. The axially symmetric monoenergetic electron bunch flies into the waveguide through this wall, and then it moves with constant velocity v_0 along the z axis. We neglect the necessity of presence of vacuum transit channel and its influence on waveguide electrodynamics, and for simplification of calculations the dielectric filling is considered to be solid.

For determination of field, excited by the bunch with arbitrary distribution of density, it is necessary to find at first the field of infinitely thin and short charged ring, coaxial with the waveguide. The densities of charge ρ and current $\mathbf{j}$ of such ring in the case of uniform straight-line motion are

$$\rho = -\frac{q}{2\pi r_0 v_0}\delta(r-r_0)\,\delta(t-t_L),$$

$$\mathbf{j} = \rho v_0 \mathbf{e}_z, \tag{1}$$

where $-q$ is the charge of the ring, v_0 and r_0 are, correspondingly, the constant velocity and radius of the ring, $t_L(t_0,r_0,z) = t_0 + z/v_0$ is the Lagrangian time of the ring, t_0 is the moment of ring's arrival into the waveguide, and $\mathbf{e}_z$ is the unit vector in the direction along the z axis. The bunch of finite size can be represented as a set of such annular bunches (macroparticles) with different charges, radii, and arrival times.

The electromagnetic field excited by the charge in the semi-infinite waveguide satisfies the Maxwell's equations with the source function in form (1) and the following boundary conditions:

$$E_z|_{r=b} = 0,$$

$$E_r|_{z=0} = 0. \tag{2}$$

After carrying out the Fourier transformation we obtain the following equation of excitation for the Fourier component of azimutal magnetic field H_φ^ω:

$$\left[\frac{\partial^2}{\partial r^2} + \frac{1}{r}\frac{\partial}{\partial r} - \frac{1}{r^2} + \frac{\partial^2}{\partial z^2} + \frac{\varepsilon\omega^2}{c^2}\right] H_\varphi^\omega = \frac{4\pi}{c}\frac{\partial}{\partial r} j_z^\omega, \tag{3}$$

where c is the speed of light in vacuum, and

$$j_z^\omega = -\frac{q}{4\pi^2 r_0}\delta(r-r_0)\exp(i\omega t_L).$$

Fourier components of longitudinal (E_z^ω) and radial (E_r^ω) electric fields are expressed via H_φ^ω:

$$E_z^\omega = \frac{ic}{\omega\varepsilon r}\frac{\partial}{\partial r}(rH_\varphi^\omega) - \frac{4\pi i}{\omega\varepsilon} j_z^\omega, \tag{4}$$

$$E_r^\omega = -\frac{ic}{\omega\varepsilon}\frac{\partial}{\partial z} H_\varphi^\omega. \tag{5}$$

In order to solve Eq. (3) we present H_φ^ω as a series of eigenfunctions of waveguide,

$$H_\varphi^\omega = \sum_{n=1}^{\infty} a_{\varphi n}(z,\omega) J_1\left(\lambda_n \frac{r}{b}\right), \tag{6}$$

where J_1 is the Bessel function of first kind of first order, λ_n is the nth root of the Bessel function of zero order (J_0). After substituting Eq. (6) into Eq. (3) and also taking into account Eqs. (2) and (5), we obtain the following expression for the Fourier component of azimutal magnetic field:

$$H_\varphi^\omega = \frac{2q}{\pi c b}\sum_{n=1}^{\infty} R_{1n}(r,r_0,b)\frac{\omega_{0n}^2 \exp(i\omega t_0)}{\lambda_n(\omega^2-\omega_{0n}^2)}\left[\exp(i\omega z/v_0) - \frac{\omega}{k_{zn}v_0}\exp(ik_{zn}z)\right],$$

where $R_{mn}(r,r_0,b) = J_0(\lambda_n r_0/b) J_m(\lambda_n r/b)/J_1^2(\lambda_n)$, $\omega_{0n}^2 = \lambda_n^2/(b^2\varepsilon/c^2 - b^2/v_0^2)$, $k_{zn}^2 = \varepsilon\omega^2/c^2 - \lambda_n^2/b^2$, and k_{zn} is the longitudinal wave number of nth radial harmonic of free electromagnetic oscillations in the dielectric-filled waveguide.

After carrying out the inverse Fourier transformation for H_φ^ω and taking into account Eqs. (4) and (5), we obtain

$$E_z(t,r,z,t_0,r_0) = -\frac{2q}{\pi b^2\varepsilon}\sum_{n=1}^{\infty} R_{0n}(r,r_0,b) \times\left(\frac{\partial}{\partial\tau} I_{1n} + \frac{i\omega_{0n}^2 c}{\sqrt{\varepsilon}v_0} I_{2n}\right), \tag{7}$$

$$E_r(t,r,z,t_0,r_0) = \frac{2q}{\pi b\varepsilon v_0}\sum_{n=1}^{\infty}\frac{\omega_{0n}^2}{\lambda_n} R_{1n}(r,r_0,b) \times\left(I_{1n} + i\frac{\partial}{\partial\xi} I_{2n}\right), \tag{8}$$

$$H_\varphi(t,r,z,t_0,r_0) = \frac{2q}{\pi bc}\sum_{n=1}^{\infty}\frac{\omega_{0n}^2}{\lambda_n} R_{1n}(r,r_0,b) \times\left(I_{1n} - \frac{ic}{\sqrt{\varepsilon}v_0}\frac{\partial}{\partial\tau} I_{2n}\right). \tag{9}$$

Here $\tau = t - t_0$, $\xi = z\sqrt{\varepsilon}/c$, and

$$I_{1n} = \int_{-\infty}^{+\infty} d\omega \frac{\exp(-i\omega\tau + i\omega z/v_0)}{\omega^2-\omega_{0n}^2}, \tag{10}$$

$$I_{2n} = \int_{-\infty}^{+\infty} d\omega \frac{\exp(-i\omega\tau + i\xi\sqrt{\omega^2-\alpha_n^2})}{\sqrt{\omega^2-\alpha_n^2}(\omega^2-\omega_{0n}^2)}, \tag{11}$$

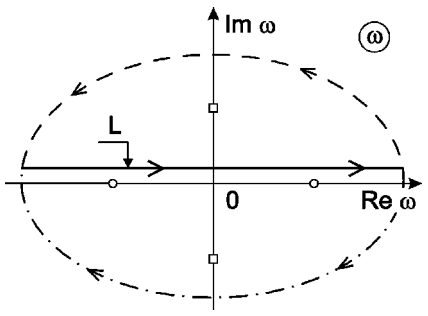

FIG. 1. Contours for calculation of integrals I_{1n}, $\tilde{I}_{1n}$ in complex plane ω. L is the initial contour of integration. Dashed line closes L if $t-t_0-z/v_0<0$, dash-dotted line closes L if $t-t_0-z/v_0>0$. Here and hereinafter white circles mark the poles $\omega=\pm\omega_{0n}$ related to the case $v_0>c/\sqrt{\varepsilon}$, and white squares mark the poles $\omega=\pm i\tilde{\omega}_{0n}$ related to the case $v_0<c/\sqrt{\varepsilon}$.

where $\alpha_n=\lambda_n c/(b\sqrt{\varepsilon})$. For the integration in Eqs. (10) and (11) it is necessary to go above the singular points at the real axis, because in this case the excited field is equal to zero in the region $z>0$ when $t<t_0$.

B. Calculation of integrals

Thus, the problem of determination of electromagnetic field is brought to the calculation of integrals (10) and (11). The process of calculation essentially depends on whether $v_0>c/\sqrt{\varepsilon}$ or $v_0<c/\sqrt{\varepsilon}$. In the first case the charged bunch is in Cherenkov resonance with eigenwaves of waveguide. besides the Cherenkov radiation the transition radiation will arise due to the presence of the boundary $z=0$. The transition radiation will interfere with the Cherenkov one. In the second case only the transition radiation will be excited, which will superimpose on the quasistatic field of uniformly moving charged bunch. The first (resonance) case is typical for dielectric wake-field accelerators. The second (nonresonance) case can be used for obtaining wideband electromagnetic pulses. In the resonance case, the term ω_{0n}^2, which appears in Eqs. (7)–(11), defines two singular points $\omega=\pm\omega_{0n}$ on the real axis. In the nonresonance case, the term ω_{0n}^2 becomes negative and it is convenient to change it for $\tilde{\omega}_{0n}^2\equiv-\omega_{0n}^2$. This substitution will define two singular points $\omega=\pm i\tilde{\omega}_{0n}$ on the imaginary axis.

Integral (10) describes the field of moving charge in the infinite waveguide. If $v_0>c/\sqrt{\varepsilon}$ this is the Cherenkov wake wave field. If $v_0<c/\sqrt{\varepsilon}$ this is simply the quasistatic field. In both cases integral (10) can be easily calculated with the help of the theorem of residues because the initial contour of integration can be transformed into the closed one by half circles of infinite radii, as is shown in Fig. 1. Integration along these half circles will give zero. Notice that, in contrast to the resonance case, the value of Eq. (10) is nonzero in front of the charge in the nonresonance case:

$$I_{1n}=\begin{cases}-\dfrac{2\pi}{\omega_{0n}}\sin[\omega_{0n}(t-t_0-z/v_0)] \\ \qquad\text{for } t-t_0-z/v_0\geqslant 0, \\ 0 \qquad\text{for } t-t_0-z/v_0<0;\end{cases} \tag{12a}$$

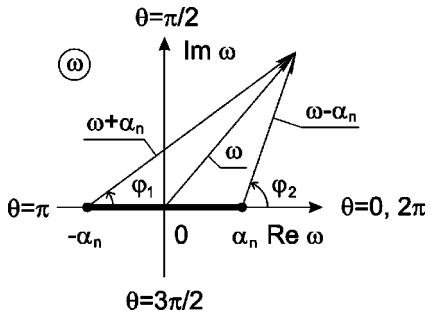

FIG. 2. The selection of branch of function $k_{zn}=(\sqrt{\varepsilon}/c)\sqrt{\omega^2-\alpha_n^2}$. $\varphi_1=\arg(\omega+\alpha_n)$, $\varphi_2=\arg(\omega-\alpha_n)$, and $\vartheta=\arg(k_{zn})=(\varphi_1+\varphi_2)/2$. Here and hereinafter black circles mark the branch points $\omega=\pm\alpha_n$, the thick line depicts the branch cut between the branch points.

$$\tilde{I}_{1n}=\begin{cases}\dfrac{\pi}{\tilde{\omega}_{0n}}\exp[-\tilde{\omega}_{0n}(t-t_0-z/v_0)] \\ \qquad\text{for } t-t_0-z/v_0\geqslant 0, \\ \dfrac{\pi}{\tilde{\omega}_{0n}}\exp[\tilde{\omega}_{0n}(t-t_0-z/v_0)] \\ \qquad\text{for } t-t_0-z/v_0<0.\end{cases} \tag{12b}$$

Integral (11) corresponds to the free electromagnetic oscillations in cylindrical waveguide. Terms with I_{2n} appeared in Eqs. (7)–(9) due to the finiteness of system along the z axis. These terms allow the fields to satisfy the boundary condition (2) at the metal plane at input end. Exact analytical solution for similar integral was found, e.g., in Refs. [14] and [15].

The function $k_{zn}=(\sqrt{\varepsilon}/c)\sqrt{\omega^2-\alpha_n^2}$ is double valued and has branch points at $\omega=\pm\alpha_n$. Make the branch cut in complex plane ω along the segment $(-\alpha_n;\ \alpha_n)$ and choose that branch of square root, which is determined by condition $0<\arg(\omega\pm\alpha_n)<2\pi$ (see Fig. 2). In this case the signs of real and imaginary parts of $k_{zn}(\omega)$ are equal to that of real and imaginary parts of ω, correspondingly. This condition must be satisfied, because we consider only the waves propagating in the positive direction of the z axis. Such waves have $\mathrm{sgn}[\mathrm{Re}(k_z)]=\mathrm{sgn}[\mathrm{Re}(\omega)]$.

Integral (11) can be easily calculated when $t-t_0-z\sqrt{\varepsilon}/c<0$. In this case the initial contour of integration L can be closed by the half circle of infinite radius in the upper complex half plane ω (see Fig. 3). Integration along this half circle gives zero. If $v_0>c/\sqrt{\varepsilon}$ there are no singular points inside the closed contour, and if $v_0<c/\sqrt{\varepsilon}$ there is one singularity, $\omega=i\tilde{\omega}_{0n}$, inside the closed contour. That is why, when $t-t_0-z\sqrt{\varepsilon}/c<0$,

$$I_{2n}=0, \tag{13a}$$

$$\tilde{I}_{2n}=-\frac{i\pi\sqrt{\varepsilon}v_0}{\tilde{\omega}_{0n}^2 c}\exp[\tilde{\omega}_{0n}(t-t_0-z/v_0)]. \tag{13b}$$

When $t-t_0-z\sqrt{\varepsilon}/c>0$, the integral along the contour C_{inf}, which is the half circle of infinite radius in the lower

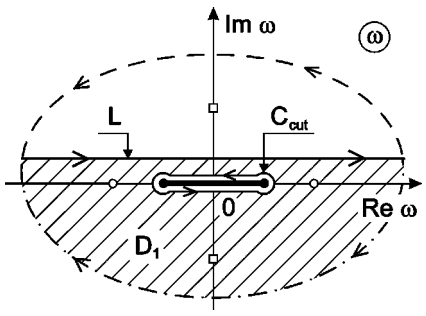

FIG. 3. Contours for calculation of integrals I_{2n}, $\tilde{I}_{2n}$ in complex plane ω. L is the initial open contour. The dashed line marks the way of closing of this contour when $t-t_0-z\sqrt{\varepsilon}/c<0$. The dash-dotted line marks the contour of infinite radius $C_{\inf}$. C_{cut} is the closed contour, which encloses the branch cut $(-\alpha_n;\alpha_n)$. Region D_1 is hatched.

half plane ω, is equal to zero. After closing the initial contour L by contour $C_{\inf}$, we obtain the domain D_1 that contains the branch cut $(-\alpha_n\ ;\alpha_n)$. We transform D_1 into the doubly connected domain by including contour C_{cut} into its boundary, as is depicted in Fig. 3. According to the theorem of residues

$$I_{2n}+I_{\text{cut}}=-2\pi i[\operatorname{Res}F(-\omega_{0n})+\operatorname{Res}F(\omega_{0n})], \tag{14a}$$

$$\tilde{I}_{2n}+\tilde{I}_{\text{cut}}=-2\pi i\operatorname{Res}F(-i\tilde{\omega}_{0n}). \tag{14b}$$

Here I_{cut} and $\tilde{I}_{\text{cut}}$ are the integrals along the contour C_{cut}, and $\operatorname{Res}F(\omega_0)$ denotes the residue of subintegral function in Eq. (11) at corresponding singularity ω_0. For determination of integrals along the banks of branch cut we consider the doubly connected domain D_2^{ω}, represented in Fig. 4. Contour C_{cut} is the inner boundary of D_2^{ω}. The outer boundary of D_2^{ω} is ellipse C_{el}^{ω}, focuses of which are situated at the branch points $\omega=\pm\alpha_n$. The equation of C_{el}^{ω} is

$$\frac{(\operatorname{Re}\omega)^2}{X^2}+\frac{(\operatorname{Im}\omega)^2}{Y^2}=1, \tag{15}$$

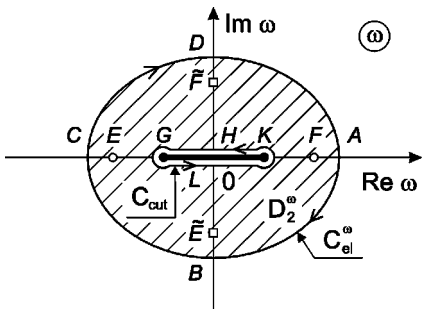

FIG. 4. Doubly connected domain D_2^{ω} (hatched). C_{el}^{ω} is the elliptic contour (15). Letters A–L mark the typical points of region D_2^{ω} in order to trace its transformation on the subsequent figures.

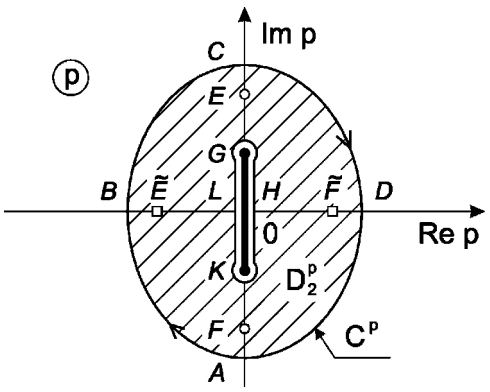

FIG. 5. Hatched region D_2^p in complex plane p is the image of D_2^{ω} after the transformation $p=-i\omega$.

where $X^2-Y^2=\alpha_n^2$. In the case $v_0>c/\sqrt{\varepsilon}$, it must be $X>\omega_{0n}$, and in the case $v_0<c/\sqrt{\varepsilon}$, it must be $Y>\tilde{\omega}_{0n}$. The direction of circulation of contour C_{el}^{ω} is negative. According to the theorem of residues,

$$I_{cut}+I_{el}=-2\pi i[\operatorname{Res}F(-\omega_{0n})+\operatorname{Res}F(\omega_{0n})], \tag{16a}$$

$$\tilde{I}_{cut}+\tilde{I}_{el}=-2\pi i[\operatorname{Res}F(-i\tilde{\omega}_{0n})+\operatorname{Res}F(i\tilde{\omega}_{0n})], \tag{16b}$$

where I_{el} and $\tilde{I}_{el}$ are integrals along the contour C_{el}^{ω}. Comparing Eqs. (14) and (16) we obtain

$$I_{2n}=I_{el}, \tag{17a}$$

$$\tilde{I}_{2n}=\tilde{I}_{el}-\frac{i\pi\sqrt{\varepsilon}v_0}{\tilde{\omega}_{0n}^2c}\exp[\tilde{\omega}_{0n}(t-t_0-z/v_0)]. \tag{17b}$$

The second term in Eq. (17b) corresponds to the residue at singularity $i\tilde{\omega}_{0n}$. Expressions (17) allow to pass from integration along the infinite straight line L to integration along the closed contour C_{el}^{ω}.

The calculation of I_{el} in the case $v_0>c/\sqrt{\varepsilon}$ and the calculation of $\tilde{I}_{el}$ in the case $v_0<c/\sqrt{\varepsilon}$ are almost identical. The difference is that the line, along which the singularities of first order are situated if $v_0>c/\sqrt{\varepsilon}$, is perpendicular to the line along which similar singularities are situated if $v_0<c/\sqrt{\varepsilon}$. That is why we describe below only the procedure of calculation of I_{el}.

Let us change the variable $p=-i\omega$. This results in $\pi/2$ turn of domain D_2^{ω} relative to the point $\omega=0$ (see Fig. 5). Contour C_{el}^{ω} transforms into the contour C^p in complex plane p. The equation of C^p is

$$\frac{(\operatorname{Re}p)^2}{Y^2}+\frac{(\operatorname{Im}p)^2}{X^2}=1.$$

The direction of circulation of C^p is negative. Expression for I_{el} is

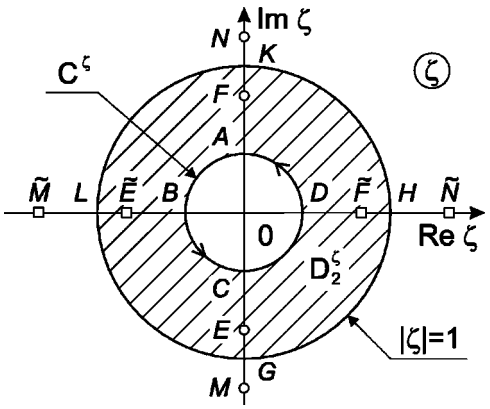

FIG. 6. Hatched region D_2^ζ is obtained from D_2^p after transformation $\zeta=(\sqrt{p^2+\alpha_n^2}-p)/\alpha_n$. Points M, N, and $\tilde{M}$, $\tilde{N}$ mark the additional couples of poles that appear in the subintegral function.

$$I_{el}=\int_{C^p} dp \frac{-\exp(p\tau-\xi\sqrt{p^2+\alpha_n^2})}{\sqrt{p^2+\alpha_n^2}(p^2+\omega_{0n}^2)}.$$

Next variable is $\zeta=(\sqrt{p^2+\alpha_n^2}-p)/\alpha_n$. Function $\zeta(p)$ is double valued, so we choose that branch of function where $0<\arg(p\pm i\alpha_n)<2\pi$. In this case the signs of real and imaginary parts of square root will coincide with the signs of real and imaginary parts of p. Such function transforms the banks of branch cut $(-i\alpha_n;i\alpha_n)$ into the circle with unitary radius in complex plane ζ, and the elliptic contour C^p into the circular contour C^ζ (see Fig. 6). Direction of circulation of contour C^ζ is positive. The equation of C^ζ is

$$(\mathrm{Re}\,\zeta)^2+(\mathrm{Im}\,\zeta)^2=\frac{(X-Y)^2}{\alpha_n^2}.$$

The integral transforms in the following way:

$$I_{el}=\frac{4}{\alpha_n^2}\int_{C^\zeta} d\zeta \frac{\zeta\exp\left\{-\frac{\alpha_n}{2}\left[\zeta(\tau+\xi)-\frac{\tau-\xi}{\zeta}\right]\right\}}{(\zeta-\zeta_1)(\zeta-\zeta_2)(\zeta-\zeta_3)(\zeta-\zeta_4)},$$

where $\zeta_1=i[(\sqrt{\varepsilon}v_0-c)/(\sqrt{\varepsilon}v_0+c)]^{1/2}$, $\zeta_2=i[(\sqrt{\varepsilon}v_0+c)/(\sqrt{\varepsilon}v_0-c)]^{1/2}$, $\zeta_3=-\zeta_1$, and $\zeta_4=-\zeta_2$. The appeared additional couple of singularities is situated beyond the unitary circle, because $(X-Y)/\alpha_n<|\zeta_1|$. So, inside the contour C^ζ there is only one singular point $\zeta=0$.

Let us make the last change of variable $\zeta=-\beta w$, where $\beta=\sqrt{(\tau-\xi)/(\tau+\xi)}$. Contour C^ζ transforms into the circular contour C^w with positive direction of circulation (see Fig. 7). The equation of C^w is

$$(\mathrm{Re}\,w)^2+(\mathrm{Im}\,w)^2=\frac{(X-Y)^2}{\beta^2\alpha_n^2}.$$

Inside the contour C^w only one singular point $w=0$ is contained. The integral takes the form

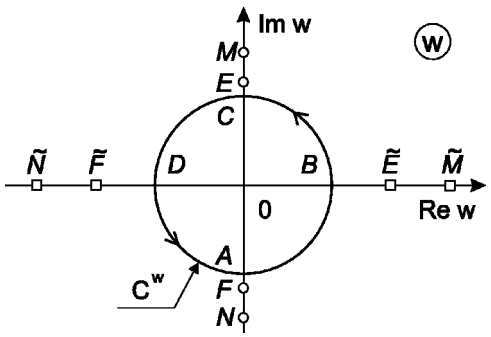

FIG. 7. Final form of integration contour C^w in complex plane w, into which contour C^ζ transforms after substitution $\zeta=-\beta w$.

$$I_{el}=\frac{4}{\alpha_n^2\beta^2}\int_{C^w} dw \frac{w\exp\left[\frac{1}{2}\left(w-\frac{1}{w}\right)\alpha_n\sqrt{\tau^2-\xi^2}\right]}{(w-w_1)(w-w_2)(w-w_3)(w-w_4)},$$

where $w_{1,2,3,4}=\zeta_{1,2,3,4}/\beta$, respectively. The subintegral function can be transformed as follows:

$$I_{el}=\frac{\sqrt{\varepsilon}v_0}{2\omega_{0n}^2c}\int_{C^w} dw \exp\left[\frac{\alpha_n\sqrt{\tau^2-\xi^2}}{2}\left(w-\frac{1}{w}\right)\right] \times\left\{\frac{1}{w-w_1}-\frac{1}{w-w_2}+\frac{1}{w-w_3}-\frac{1}{w-w_4}\right\}. \quad (18)$$

As the contour C^w does not contain the singularities $w=w_{1,2,3,4}$, at this contour the following expansions are valid:

$$-\frac{1}{w-w_j}=\frac{1}{w_j}\sum_{k=0}^{\infty}\left(\frac{w}{w_j}\right)^k, \quad (19)$$

where $j=1,2,3,4$. Let us notice also that [16]

$$\frac{1}{2\pi i}\int_{C^w} dw\, w^k \exp\left[\frac{x}{2}\left(w-\frac{1}{w}\right)\right]=(-1)^{k+1}J_{k+1}(x). \quad (20)$$

After substituting series (19) into (18), interchanging the order of integration and summation, and taking into account Eq. (20), we obtain

$$I_{el}=\frac{2\pi i\sqrt{\varepsilon}v_0}{\omega_{0n}^2c}\sum_{m=0}^{\infty}(-1)^m(r_2^{2+2m}-r_1^{2+2m})J_{2+2m}(y_n), \quad (21)$$

where $r_1=\beta[(\sqrt{\varepsilon}v_0-c)/(\sqrt{\varepsilon}v_0+c)]^{1/2}$, $r_2=\beta[(\sqrt{\varepsilon}v_0+c)/(\sqrt{\varepsilon}v_0-c)]^{1/2}$, $y_n=\alpha_n\sqrt{\tau^2-\xi^2}$.

The Lommel function of the nth order of two arguments $U_n(q,x)$ is defined as [17]

$$U_n(q,x)=\sum_{m=0}^{\infty}(-1)^m\left(\frac{q}{x}\right)^{n+2m}J_{n+2m}(x). \quad (22)$$

Finally, after taking into account (17), (21), and (22), we can write in resonance and nonresonance cases for $t-t_0-z\sqrt{\varepsilon}/c>0$:

$$I_{2n}=\frac{2\pi i\sqrt{\varepsilon}v_0}{\omega_{0n}^2 c}[U_2(r_2 y_n,y_n)-U_2(r_1 y_n,y_n)], \quad (23a)$$

$$\tilde{I}_{2n}=-\frac{2\pi i\sqrt{\varepsilon}v_0}{\tilde{\omega}_{0n}^2 c}\left\{U_2(i\tilde{r}_2 y_n,y_n)-U_2(i\tilde{r}_1 y_n,y_n)+\frac{1}{2}\exp[\tilde{\omega}_{0n}(t-t_0-z/v_0)]\right\}, \quad (23b)$$

where $\tilde{r}_{1,2}^2\equiv -r_{1,2}^2$, respectively.

C. Some properties of Lommel functions

Now the integrals I_{1n} and I_{2n} are calculated. But before one will turn to Eqs. (7)–(9), let us notice, first, that using the properties of Lommel functions [17] the following necessary expression must be obtained:

$$\frac{d}{dx}U_n(ry,y)=\frac{d}{dx}\left(\frac{ry}{2}+\frac{y}{2r}\right)U_{n-1}(ry,y)-\frac{d}{dx}\left(\frac{y}{r}\right)\frac{r^{n-1}}{2}J_{n-1}(y), \quad (24)$$

where $r=r(x)$, $y=y(x)$. Second, if $|q|\leqslant|x|$, the Lommel function $U_n(q,x)$ can be easily calculated with the help of Eq. (22). If $|q|>|x|$, the number of members m of series in Eq. (22), which must be accounted for obtaining the converging result, is approximately defined by condition $n+2m>x$, that is why in the case of big $|x|\gg 1$ the direct summation of series (22) seems to be rather problematic. Hence, if $|x|>1$, the following property of Lommel functions must be used [17]:

$$U_n(q,x)=\cos\left(\frac{q}{2}+\frac{x^2}{2q}-\frac{n\pi}{2}\right)+\sum_{m=0}^{\infty}(-1)^{n+m}\left(\frac{x}{q}\right)^{-n+2+2m}\times J_{-n+2+2m}(x). \quad (25)$$

One can show analytically that when $x=q$, formulas (22) and (25) can be transformed to the identical expressions. As we are interested in functions with $n=1$ and $n=2$, finally we write that

$$U_2(ry,y)=\begin{cases}-\sum_{m=1}^{\infty}(-1)^m r^{2m}J_{2m}(y) & \text{if } |r|\leqslant 1,\\ -\cos\left(\frac{ry}{2}+\frac{y}{2r}\right)+\sum_{m=0}^{\infty}\frac{(-1)^m}{r^{2m}}J_{2m}(y) & \text{if } |r|>1;\end{cases} \quad (26)$$

$$U_1(ry,y)=\begin{cases}\sum_{m=0}^{\infty}(-1)^m r^{1+2m}J_{1+2m}(y) & \text{if } |r|\leqslant 1,\\ \sin\left(\frac{ry}{2}+\frac{y}{2r}\right)-\sum_{m=0}^{\infty}\frac{(-1)^m}{r^{1+2m}}J_{1+2m}(y) & \text{if } |r|>1.\end{cases} \quad (27)$$

We shall need also the following relations:

$$\frac{r_2 y_n}{2}+\frac{y_n}{2r_2}\equiv\omega_{0n}(t-t_0-z/v_0), \quad (28a)$$

$$\frac{i\tilde{r}_2 y_n}{2}+\frac{y_n}{2i\tilde{r}_2}\equiv i\tilde{\omega}_{0n}(t-t_0-z/v_0). \quad (28b)$$

Let us introduce $v_{\mathrm{pr}}=c/\sqrt{\varepsilon}$ and $v_{\mathrm{gr}}=c^2/\varepsilon v_0$. When $t-t_0-z/v_{\mathrm{pr}}\geqslant 0$ we have

$$0\leqslant r_1<1,$$

$$0\leqslant r_2\leqslant 1 \quad \text{for } t-t_0-z/v_{\mathrm{gr}}\leqslant 0, \quad (29a)$$

$$r_2>1 \quad \text{for } t-t_0-z/v_{\mathrm{gr}}>0;$$

$$0\leqslant\tilde{r}_1<1,$$

$$0\leqslant\tilde{r}_2\leqslant 1 \quad \text{for } t-t_0-z/v_0\leqslant 0, \quad (29b)$$

$$\tilde{r}_2>1 \quad \text{for } t-t_0-z/v_0>0.$$

Inequalities (29) define the regions where the various presentations (26), (27) of Lommel functions will be used for the field structure description. In the case $v_0>c/\sqrt{\varepsilon}$ the harmonic terms in Eqs. (26) and (27) will give the electromagnetic wave that will be equal to the Cherenkov wake wave, but with the opposite sign. This is the so-called ''quenching wave'' [9], which compensates the Cherenkov radiation field in the region $0<z<(t-t_0)v_{\mathrm{gr}}$. In the case $v_0<c/\sqrt{\varepsilon}$ the sine and cosine in Eqs. (26), (27) will become the hyperbolic ones and will compensate the exponentially growing term in Eq. (23b) in the region $0<z<(t-t_0)v_0$.

D. Final expressions for the field in resonance case

In order to obtain the expressions describing the excited fields, one must substitute Eqs. (12), (13), and (23) into Eqs. (7)–(9) by taking into account Eqs. (24) and (26)–(29).

In the case of Cherenkov resonance the field, excited by the thin charged ring (1) in the semi-infinite waveguide, can be written, similar to Ref. [9], in the form of superposition of spatially limited Cherenkov radiation field and transition radiation field. The longitudinal electric field:

$$E_z(t,r,z,t_0,r_0)=E_z^{\mathrm{Cher}}(t,r,z,t_0,r_0)+E_z^{\mathrm{trans}}(t,r,z,t_0,r_0), \tag{30}$$

$$E_z^{\mathrm{Cher}}(t,r,z,t_0,r_0)=\frac{4q}{b^2\varepsilon}\sum_{n=1}^{\infty}R_{0n}(r,r_0,b)\cos[\omega_{0n}(t-t_0-z/v_0)]\vartheta[z,(t-t_0)v_{\mathrm{gr}},(t-t_0)v_0], \tag{31}$$

$$E_z^{\mathrm{trans}}(t,r,z,t_0,r_0)=\frac{4q}{b^2\varepsilon}\sum_{n=1}^{\infty}R_{0n}(r,r_0,b)\Bigg\{\vartheta[z,(t-t_0)\times v_{\mathrm{gr}},(t-t_0)v_{\mathrm{pr}}]\sum_{m=1}^{\infty}(-1)^m(r_1^{2m}-r_2^{2m})\times J_{2m}(y_n)+\vartheta[z,0,(t-t_0)v_{\mathrm{gr}}]\Bigg[J_0(y_n)+\sum_{m=1}^{\infty}(-1)^m\left(r_1^{2m}+\frac{1}{r_2^{2m}}\right)J_{2m}(y_n)\Bigg]\Bigg\}. \tag{32}$$

The function ϑ is defined as

$$\vartheta(z,z_1,z_2)=\begin{cases}1 & \text{if } z_1\leqslant z<z_2\\ 0 & \text{if } z<z_1 \quad \text{or} \quad z_2\leqslant z.\end{cases}$$

The radial electric field:

$$E_r(t,r,z,t_0,r_0)=E_r^{\mathrm{Cher}}(t,r,z,t_0,r_0)+E_r^{\mathrm{trans}}(t,r,z,t_0,r_0), \tag{33}$$

$$E_r^{\mathrm{Cher}}(t,r,z,t_0,r_0)=-\frac{4q}{b^2\varepsilon\sqrt{\varepsilon v_0^2/c^2-1}}\sum_{n=1}^{\infty}R_{1n}(r,r_0,b)\times\sin[\omega_{0n}(t-t_0-z/v_0)]\vartheta[z,(t-t_0)v_{\mathrm{gr}},(t-t_0)v_0], \tag{34}$$

$$E_r^{\mathrm{trans}}(t,r,z,t_0,r_0)=\frac{4q}{b^2\varepsilon\sqrt{\varepsilon v_0^2/c^2-1}}\sum_{n=1}^{\infty}R_{1n}(r,r_0,b)\times\Bigg\{\vartheta[z,(t-t_0)v_{\mathrm{gr}},(t-t_0)v_{\mathrm{pr}}]\times\sum_{m=0}^{\infty}(-1)^m(r_1^{1+2m}+r_2^{1+2m})\times J_{1+2m}(y_n)+\vartheta[z,0,(t-t_0)v_{\mathrm{gr}}]\times\times\sum_{m=0}^{\infty}(-1)^m\left(r_1^{1+2m}-\frac{1}{r_2^{1+2m}}\right)\times J_{1+2m}(y_n)\Bigg\}. \tag{35}$$

The azimutal magnetic field:

$$H_\varphi(t,r,z,t_0,r_0)=H_\varphi^{\mathrm{Cher}}(t,r,z,t_0,r_0)+H_\varphi^{\mathrm{trans}}(t,r,z,t_0,r_0), \tag{36}$$

$$H_\varphi^{\mathrm{Cher}}(t,r,z,t_0,r_0)=-\frac{4qv_0}{b^2\sqrt{\varepsilon v_0^2-c^2}}\sum_{n=1}^{\infty}R_{1n}(r,r_0,b)\times\sin[\omega_{0n}(t-t_0-z/v_0)]\times\vartheta[z,(t-t_0)v_{\mathrm{gr}},(t-t_0)v_0], \tag{37}$$

$$H_\varphi^{\mathrm{trans}}(t,r,z,t_0,r_0)=-\frac{4qv_0}{b^2\sqrt{\varepsilon v_0^2-c^2}}\sum_{n=1}^{\infty}R_{1n}(r,r_0,b)\times\Bigg\{\vartheta[z,(t-t_0)v_{\mathrm{gr}},(t-t_0)v_{\mathrm{pr}}]\times\sum_{m=0}^{\infty}(-1)^m(r_1^{1+2m}-r_2^{1+2m})\times J_{1+2m}(y_n)+\vartheta[z,0,(t-t_0)v_{\mathrm{gr}}]\times\sum_{m=0}^{\infty}(-1)^m\left(r_1^{1+2m}+\frac{1}{r_2^{1+2m}}\right)\times J_{1+2m}(y_n)\Bigg\}. \tag{38}$$

Cherenkov components (31), (34), and (37) are written by taking into account the quenching wave and are nonzero when $(t-t_0)v_{\mathrm{gr}}\leqslant z<(t-t_0)v_0$. Within the limits of this region the amplitude of each harmonic of Cherenkov component is constant [see Fig. 8(b)]. The value v_{gr} is the group velocity of electromagnetic wave, which is synchronous with the charge. Plane $z_{\mathrm{gr}}=(t-t_0)v_{\mathrm{gr}}$ is the "group wave front" of wake field. This wave front moves behind the bunch with group velocity v_{gr}.

Transition components (32), (35), and (38) exist in the region $0\leqslant z<(t-t_0)v_{\mathrm{pr}}$. The value v_{pr} is the maximal velocity of propagation of electromagnetic signals in dielectric-filled waveguide. Exactly with this velocity the fastest high-frequency part of transition radiation—the so-called precursor [11]—propagates. The envelope of each harmonic of transition component is maximal near the group wave front [line *A* in Fig. 8] and decreases as one moves away from it. In precursor [line *B* in Fig. 8(c)] it tends to zero, coordinate of precursor is $z_{\mathrm{pr}}=(t-t_0)v_{\mathrm{pr}}$. Near the metal end wall the envelope of E_z is small, but nonzero and it decreases with time. Transition components undergo a sudden discontinuous change at the plane of group wave front [see Fig. 8(c)]. This occurs due to the fact that we artificially split the continuous total field [Eqs. (30), (33), and (36)] into components, and the separated Cherenkov component [Eqs. (31), (34), (37)] turns to zero abruptly also when crossing the plane of group wave front, as it is shown in Fig. 8(b).

As a result, at certain moment of time t the spatial pattern of single harmonic of total field looks like that represented in Fig. 8(a). In front of the bunch (line *C*) the field is equal to

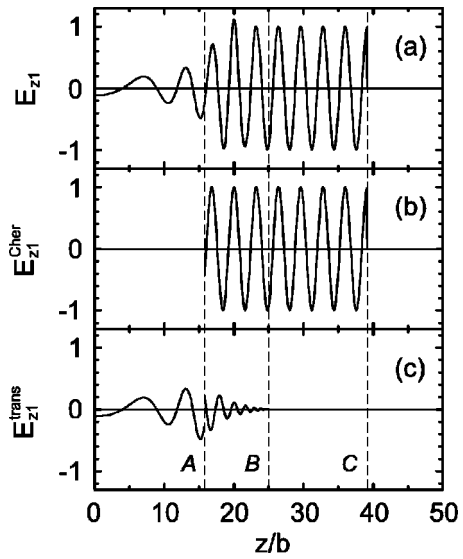

FIG. 8. Longitudinal structure of the first harmonic of the longitudinal electric field (in relative units) given by Eqs. (30)–(32) in the fixed moment of time. (a) Total field, (b) Cherenkov component, and (c) transition component. Line *A* marks the position of the group wave front, line *B* marks the position of the precursor, and line *C* marks the position of the charge. $tc/b=40$, $r/b=0$, $t_0=0$, $v_0/c=0.9798$, $\varepsilon=2.6$.

zero. To the left from precursor's position z_{pr} (line *B*) the field's envelope disturbs and starts to decrease, at group wave front (line *A*) it is equal to the half of Cherenkov amplitude. In the region $z \ll z_{gr}$ the field is small and it decreases with time.

E. Final expressions for the field in nonresonance case

In the case when the Cherenkov resonance condition is not satisfied, we write the field, excited by the thin ring-shaped charge (1), in the form of superposition of quasistatic field of uniformly moving charged ring and field of transition radiation. The longitudinal electric field:

$$E_z(t,r,z,t_0,r_0)=E_z^{\mathrm{qstat}}(t,r,z,t_0,r_0)+E_z^{\mathrm{trans}}(t,r,z,t_0,r_0), \tag{39}$$

$$\begin{aligned} E_z^{\mathrm{qstat}}&(t,r,z,t_0,r_0) \\ &=\frac{2q}{b^2\varepsilon}\sum_{n=1}^{\infty} R_{0n}(r,r_0,b)\{-\exp[\tilde{\omega}_{0n}(t-t_0-z/v_0)] \\ &\quad\times\vartheta[z,(t-t_0)v_0,(t-t_0)v_{\mathrm{pr}}] \\ &\quad+\exp[-\tilde{\omega}_{0n}(t-t_0-z/v_0)] \\ &\quad\times\vartheta[z,0,(t-t_0)v_0]\}, \end{aligned} \tag{40}$$

$$\begin{aligned} E_z^{\mathrm{trans}}&(t,r,z,t_0,r_0) \\ &=-E_z^{\mathrm{qstat}}(t,r,z,t_0,r_0)+\frac{4q}{b^2\varepsilon}\sum_{n=1}^{\infty} R_{0n}(r,r_0,b) \\ &\quad\times\Bigg\{\vartheta[z,(t-t_0)v_0,(t-t_0)v_{\mathrm{pr}}] \\ &\quad\times\sum_{m=1}^{\infty}(\tilde{r}_1^{2m}-\tilde{r}_2^{2m})J_{2m}(y_n)+\vartheta[z,0,(t-t_0)v_0] \\ &\quad\times\left[J_0(y_n)+\sum_{m=1}^{\infty}\left(\tilde{r}_1^{2m}+\frac{1}{\tilde{r}_2^{2m}}\right)J_{2m}(y_n)\right]\Bigg\}. \end{aligned} \tag{41}$$

The radial electric field:

$$E_r(t,r,z,t_0,r_0)=E_r^{\mathrm{qstat}}(t,r,z,t_0,r_0)+E_r^{\mathrm{trans}}(t,r,z,t_0,r_0), \tag{42}$$

$$\begin{aligned} E_r^{\mathrm{qstat}}&(t,r,z,t_0,r_0)=-\frac{2q}{b^2\varepsilon\sqrt{1-\varepsilon v_0^2/c^2}} \\ &\quad\times\sum_{n=1}^{\infty} R_{1n}(r,r_0,b)\{\exp[\tilde{\omega}_{0n}(t-t_0 \\ &\quad-z/v_0)]\vartheta[z,(t-t_0)v_0,(t-t_0)v_{\mathrm{pr}}] \\ &\quad+\exp[-\tilde{\omega}_{0n}(t-t_0-z/v_0)] \\ &\quad\times\vartheta[z,0,(t-t_0)v_0]\}, \end{aligned} \tag{43}$$

$$\begin{aligned} E_r^{\mathrm{trans}}&(t,r,z,t_0,r_0)=-E_r^{\mathrm{qstat}}(t,r,z,t_0,r_0) \\ &\quad+\frac{4q}{b^2\varepsilon\sqrt{1-\varepsilon v_0^2/c^2}}\sum_{n=1}^{\infty} R_{1n}(r,r_0,b) \\ &\quad\times\Bigg\{\vartheta[z,(t-t_0)v_0,(t-t_0)v_{\mathrm{pr}}] \\ &\quad\times\sum_{m=0}^{\infty}(\tilde{r}_1^{1+2m}-\tilde{r}_2^{1+2m})J_{1+2m}(y_n) \\ &\quad+\vartheta[z,0,(t-t_0)v_0]\sum_{m=0}^{\infty}\left(\tilde{r}_1^{1+2m} \\ &\quad-\frac{1}{\tilde{r}_2^{1+2m}}\right)J_{1+2m}(y_n)\Bigg\}. \end{aligned} \tag{44}$$

The azimutal magnetic field:

$$H_\varphi(t,r,z,t_0,r_0)=H_\varphi^{\mathrm{qstat}}(t,r,z,t_0,r_0)+H_\varphi^{\mathrm{trans}}(t,r,z,t_0,r_0), \tag{45}$$

$$\begin{aligned} H_\varphi^{\mathrm{qstat}}&(t,r,z,t_0,r_0)=-\frac{2qv_0}{b^2\sqrt{c^2-\varepsilon v_0^2}}\sum_{n=1}^{\infty} R_{1n}(r,r_0,b) \\ &\quad\times\{\exp[\tilde{\omega}_{0n}(t-t_0-z/v_0)]\vartheta[z,(t \\ &\quad-t_0)v_0,(t-t_0)v_{\mathrm{pr}}]+\exp[-\tilde{\omega}_{0n}(t-t_0 \\ &\quad-z/v_0)]\vartheta[z,0,(t-t_0)v_0]\}, \end{aligned} \tag{46}$$

$$H_{\varphi}^{\mathrm{trans}}(t,r,z,t_0,r_0) = -H_{\varphi}^{\mathrm{qstat}}(t,r,z,t_0,r_0) - \frac{4qv_0}{b^2\sqrt{c^2-\varepsilon v_0^2}} \sum_{n=1}^{\infty} R_{1n}(r,r_0,b) \times \Bigg\{ \vartheta[z,(t-t_0)v_0,(t-t_0)v_{\mathrm{pr}}] \times \sum_{m=0}^{\infty} (\tilde{r}_1^{1+2m}+\tilde{r}_2^{1+2m}) J_{1+2m}(y_n) + \vartheta[z,0,(t-t_0)v_0] \times \sum_{m=0}^{\infty} \left(\tilde{r}_1^{1+2m} + \frac{1}{\tilde{r}_2^{1+2m}} \right) J_{1+2m}(y_n) \Bigg\}. \quad (47)$$

We defined quasistatic [Eqs. (40), (43), and (46)], and transition [Eqs. (41), (44), and (47)] components of field as nonzero in the region $0 \leqslant z < (t-t_0)v_{\mathrm{pr}}$. As in the waveguide the electromagnetic signal cannot propagate with the velocity higher than v_{pr}, at the moment of time $t > t_0$ neither quasistatic, nor transition radiation fields exist in front of the point z_{pr}. At the same time, as the velocity of charge $v_0 < v_{\mathrm{pr}}$, the excited field outruns the charge in contrast with the Cherenkov resonance case. In order to illustrate the qualitative picture of propagation of radiation in the nonresonance case, the longitudinal distributions of first harmonic of total radial electric field and its Coulomb and transition components are represented in Fig. 9.

Even in the structure of single harmonic the wide set of frequencies can be observed and the most short-wavelength and high-frequency oscillations are in the precursor region. The amplitude of oscillations decreases as one moves to the precursor, and at the point $z = z_{\mathrm{pr}}$ (line *B* in Fig. 9) the total field becomes zero.

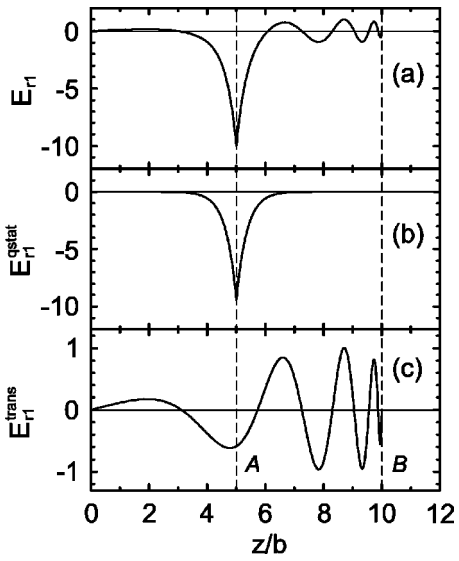

FIG. 9. Longitudinal structure of the first harmonic of the radial electric field (in relative units) given by Eqs. (42)–(44) in the fixed moment of time. (a) Total field, (b) quasistatic (Coulomb) component, and (c) transition component. Line *A* marks the position of charge, line *B* marks the position of precursor. $tc/b = 10$, $r/b = 0.25$, $t_0 = 0$, $v_0/c = 0.5$, $\varepsilon = 1$.

III. FIELD TOPOGRAPHY OF FINITE-SIZE ELECTRON BUNCH

Expressions (30)–(47) allow us to investigate the spatial structure of electromagnetic field in the semi-infinite waveguide. Notice that the sums over index *n* in these formulas are divergent, because they describe the field of the charge, whose density is determined by the δ function. The divergence is removed if one sums the contributions from all macroparticles that form the finite-size bunch. For subsequent numerical calculations, we have chosen the electron bunch with the distribution of current density,

$$j_z(r_0,t_0) = j_0 J_0\left(\lambda_1 \frac{r_0}{R_b}\right) \exp\left[-4\left(\frac{2t_0}{T_b}-1\right)^2\right], \quad (48)$$

where j_0 is the maximal value of current density, $0 \leqslant t_0 \leqslant T_b$, T_b is the bunch duration ($T_b = L_b/v_0$, where L_b is the length and v_0 is the bunch velocity), $0 \leqslant r_0 \leqslant R_b$, and R_b is the bunch radius.

Consider at first the Cherenkov resonance case. In Fig. 10(a) with the help of level curves the 2D (in the plane z-r) picture of distribution of longitudinal electric field excited by relativistic electron bunch with density (48) is represented (see the parameters in caption of Fig. 10). The bunch sizes are small in comparison with those of waveguide, so we can think that position of group wave front is $z_{\mathrm{gr}} \approx 15.6$ cm, coordinate of precursor is $z_{\mathrm{pr}} \approx 24.8$ cm, and bunch coordinate is $z_b \approx 38.7$ cm. In the region $z_{\mathrm{pr}} < z < z_b$ the intense Cherenkov wake wave exists. Structure of this wave is formed as a result of periodic reflections of Cherenkov cone from the sidewalls of waveguide. The angle at the vertex of this cone,

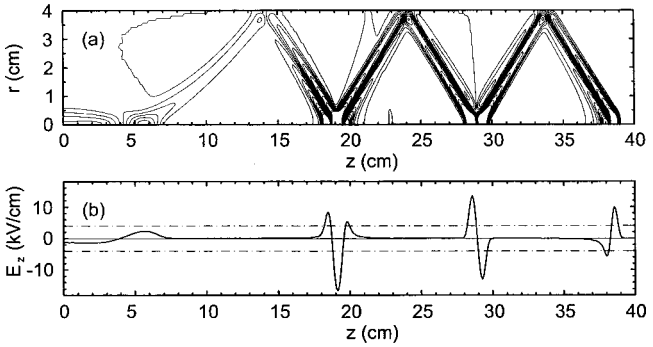

FIG. 10. Topography of field E_z in the semi-infinite waveguide in the case of Cherenkov resonance. (a) Level curves of field E_z and (b) respective dependence of E_z vs z obtained at $r = 0$. Level curves of field are drawn with a step of 0.4 kV/cm in the range from -4 kV/cm to 4 kV/cm. Dash-dotted lines in (b) mark the limits of this range. The electron bunch moves from left to right. 20 radial harmonics are taken into account. The moment of observation $tc/b = 10$. System's parameters: $b = 4$ cm, $\varepsilon = 2.6$, $L_b = 1$ cm, $R_b = 0.5$ cm, $v_0/c = 0.9798$, and bunch charge $Q = 1.6$ nC.

determined directly from the picture, equals to $\alpha \approx 39°$ that coincides with theoretical value for infinite dielectric $\alpha = \arcsin[c/(\sqrt{\varepsilon} v_0)] = 39.27°$. Note that in order to obtain the Cherenkov cone the big number of radial harmonics must be summed in Eqs. (30)–(38), as it was pointed in Ref. [3]. Conical structure of Cherenkov field in dielectric waveguide was mentioned in Ref. [7] and 2D pictures were presented in Ref. [4] for the waveguide with vacuum transit channel. But in these works infinite systems were considered. And in the semi-infinite waveguide in the region $0 < z < z_{\rm pr}$ the transition radiation field superimposes on the Cherenkov field. Weak transition oscillations in the precursor region 20 cm $< z <$ 23 cm still can be noticed against the intense Cherenkov field. Behind $z_{\rm gr}$ the field is small and its structure is different from that of the Cherenkov wave. The transition radiation field will be described in details hereinafter. In Fig. 10(b), for comparison, the respective dependence of E_z vs z at the axis of waveguide ($r = 0$) is represented. Note the high amplitude and small width of field spikes. E_z is maximal at the waveguide's axis, where the waves, reflected from sidewalls, are focusing. It is evident that for the purpose of acceleration one can use the fields in the paraxial region $r < 0.5$ cm, and in the moment of time depicted in Fig. 10 the accelerated particle must be behind the leading bunch not farther than $38.7 - 18 = 20.7$ cm.

Now study the case when there is no Cherenkov resonance. To satisfy this condition we considered the vacuum waveguide. The corresponding 2D picture of level curves of radial electric field E_r excited by electron bunch with density (48) is represented in Fig. 11(a). The profile of this picture along the line $r = 1$ cm (dependence of E_r vs z) is represented in Fig. 11(b). First of all one can notice the typical spike of Coulomb field in the region of bunch: $r < 0.5$ cm, 15 cm $< z <$ 16 cm. Amplitude of this spike is 10 kV/cm and it is much higher than the transition signal's level. But Coulomb field decays exponentially and its influence is limited by the region $r < 1.5$ cm, 14 cm $< z <$ 17 cm. One should notice also the typical convolution of level curves of transition field. The slope angle between wave front and waveguide's axis changes from 0° to 90° as one moves from the wall $z = 0$ to the precursor $z_{\rm pr} = 20$ cm. Similar behavior of transition component can be observed in Fig. 10(a). Considering the wave propagation in the waveguide as periodical reflections from the sidewalls we can conclude that the smaller is the number of reflections per unit length, the higher will be wave propagation velocity along the waveguide's axis. This velocity will be maximal when the wave propagates along the waveguide's axis or, in other words, wave front is perpendicular to the axis. That is why in the precursor region we have the fastest waves, wave front of which is almost perpendicular to the waveguide's axis [region 18 cm $< z <$ 20 cm in Fig. 11(a)]. In the region close to the wall $z = 0$ due to the boundary conditions (2) we have $E_r \to 0$, but $E_z \neq 0$. In this region ($0 < z <$ 2 cm) the slowest oscillations are localized, which fall on the sidewalls almost perpendicularly and move along the axis very slowly. Amplitude of these oscillations is very small and their frequency spectrum is determined by cutoff frequencies of the waveguide.

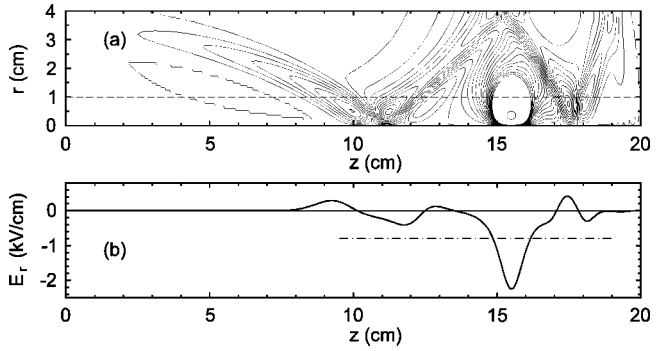

FIG. 11. Topography of field E_r in the semi-infinite waveguide in the nonresonance case. (a) Level curves of field E_r, (b) respective dependence of E_r vs z obtained at $r = 1$ cm [corresponds to dashed line in (a)]. Level curves of field are drawn with a step of 50 V/cm in the range from -800 V/cm to 800 V/cm. The dash-dotted line in (b) marks the lower limit of this range. The electron bunch moves from left to right. Twenty radial harmonics are taken into account. The moment of observation $tc/b = 5$. System's parameters: $b = 4$ cm, $\varepsilon = 1$, $L_b = 1$ cm, $R_b = 0.5$ cm, $v_0/c = 0.8$, and bunch charge $Q = 1.6$ nC.

IV. CONCLUSION

In present paper the influence of finiteness of slow-wave medium on the process of formation of electromagnetic field excited by a moving electron bunch in a semi-infinite round cylindrical dielectric-filled waveguide with metal walls has been investigated. The considered structure is a good approximation for description of real waveguide if the last one has no reflection at the output end or if the reflection is weak enough to be neglected. We made a number of nonprincipal assumptions that sufficiently simplify the process of obtaining the solution. First, the velocity of motion of charged particles is constant. Second is the absence of frequency dispersion and absorption in dielectric. Third is the solid homogeneous dielectric filling of waveguide, without vacuum transit channel. Let us note that in the case of vacuum waveguide only the first condition is necessary for the correctness of obtained solution (39)–(47). Within the limits of such approximation the exact expressions, which describe the electromagnetic field excited by the uniformly moving thin ring-shaped charge bunch in the semi-infinite waveguide, have been obtained for the cases when Cherenkov resonance condition is satisfied and when it is not. In the resonance case the field exists only behind the bunch and it is composed of spatially limited Cherenkov field, whose trailing wave front moves after the bunch with group velocity, and transition radiation. In the nonresonance case the field outruns the bunch, it composes of quasistatic field of moving charged bunch and transition radiation.

In obtained expressions the contributions from many radial harmonics with different numbers are summed. Besides that, the space and time structures of the transition component have been obtained in the form of infinite series, which can be reduced to the Lommel functions of two variables. Using the properties of Lommel functions, these series have been transformed to fast converging form, suitable for numerical analysis.

The 2D pictures of spatial distribution of field for resonance and nonresonance cases have been discussed. They demonstrated the necessity of taking into account a big number of radial harmonics, because only in this case the valid structure can be obtained. The qualitative structure of transition field is similar for both resonance and nonresonance modes—amplitude of transition field is much smaller than that of the Cherenkov or quasistatic field, the most high-frequency and short-wavelength oscillations are in the precursor.

As applied to the wake-field acceleration of charged particles in the dielectric-filled waveguide, accounting of the boundary leads to the limitation of intense accelerating field region in the longitudinal direction. The appeared effect of drift of wake field after the leading bunch will result in the following: soon after the charged bunch passed through some cross section of waveguide, the field in this cross section will tend to zero. That is why in future it is necessary to consider the influence of boundary at the output end, and to investigate multiple reflections of excited wave packet from the ends of waveguide. Besides, the absorption in dielectric must be taken into account.

Transition radiation in vacuum waveguide is of particular interest due to its properties. The impact mechanism of excitation of transition radiation by intense electron bunches can be used for generation of superwideband electromagnetic pulses. The intensity of radiation will be proportional to the squared charge of bunch [18].

[1] W. Gai, P. Schoessow, B. Cole, R. Konecny, J. Norem, J. Rosenzweig, and J. Simpson, Phys. Rev. Lett. **61**, 2756 (1988).
[2] I. Onishchenko, V. A. Kiseljov, A. K. Berezin, G. V. Sotnikov, V. V. Uskov, A. F. Linnik, and Ya. B. Fainberg, in *Proceedings of the Particle Accelerator Conference, New York, 1995* (IEEE, New York, 1995), p. 782.
[3] T. B. Zhang, J. L. Hirshfield, T. C. Marshall, and B. Hafizi, Phys. Rev. E **56**, 4647 (1997).
[4] S. Y. Park and J. L. Hirshfield, Phys. Plasmas **8**, 2461 (2001).
[5] W. Gai and P. Schoessow, Nucl. Instrum. Methods Phys. Res. A **459**, 1 (2001).
[6] V. Kiseljov, A. Linnik, V. Mirny, N. Zemliansky, R. Kochergov, I. Onishchenko, G. Sotnikov, and Ya. Fainberg, in *Proceedings of the 12th International Conference on High-Power Particle Beams, Haifa, Israel*, edited by M. Markovits and J. Shiloh (IEEE, Haifa, 1998), Vol. 2, p. 756.
[7] T. B. Zhang, T. C. Marshall, and J. L. Hirshfield, IEEE Trans. Plasma Sci. **26**, 787 (1998).
[8] B. M. Bolotovskij, Usp. Fiz. Nauk **75**, 295 (1961) [Sov. Phys. Usp. **4**, 781 (1962)].
[9] E. L. Burshtein and G. V. Voskresenskij, Zh. Tekh. Fiz. **33**, 34 (1963) [Sov. Phys. Tech. Phys. **8**, 22 (1963)].
[10] A. Sommerfeld, Ann. Phys. (Leipzig) **44**, 177 (1914).
[11] L. Brillouin, Ann. Phys. (Leipzig) **44**, 203 (1914).
[12] H. G. Baerwald, Ann. Phys. (Leipzig) **6**, 295 (1930).
[13] H. G. Baerwald, Ann. Phys. (Leipzig) **7**, 731 (1930).
[14] N. G. Denisov, Zh. Éksp. Teor. Fiz. **21**, 1354 (1951).
[15] J. R. Wait and K. P. Spies, Appl. Sci. Res. **16**, 455 (1966).
[16] M. A. Lavrent'ev and B. V. Shabat, *Methods of the Theory of Functions of Complex Variable* (Nauka, Moscow, 1973).
[17] G. N. Watson, *Treatise on the Theory of Bessel Functions* (Cambridge University Press, Cambridge, England, 1945).
[18] V. L. Ginzburg and V. N. Tsytovich, *Transition Radiation and Transient Scattering* (Nauka, Moscow, 1984).